

$^{74,76,78,80,82}\text{Se}$ by inelastic scattering of 64.8 MeV protons

Koya Ogino

Department of Nuclear Engineering, Kyoto University, Kyoto 606, Japan

(Received 12 September 1985)

The inelastic scattering of 64.8 MeV protons has been studied on the stable even $^{74-82}\text{Se}$ isotopes. The inelastically scattered protons were momentum analyzed in a magnetic spectrograph with a resulting energy resolution of approximately 20 keV. Levels up to the excitation energy of about 5 MeV were investigated. Many new levels were observed for the isotopes studied. The angular distributions obtained were compared with the predictions of distorted-wave Born approximation and coupled-channels calculations and a number of new spin assignments were proposed. Several 4^+ states with comparable strengths were found at about $E_x = 2.0-5.0$ MeV, showing large fragmentation of octupole and hexadecapole transition strengths, in contrast to the case of Zn isotopes. The distributions of the transition strengths for the 2^+ , 3^- , and 4^+ states were compared with the theoretical calculations based on the random-phase-approximation model for spherical nuclei.

I. INTRODUCTION

Nuclei from Ge to Sr, with neutrons in the $1g_{9/2}$ shell, show various interesting behavior¹ associated with the structure change around the neutron number $N = 40-42$: Studies² on $^{72-76}\text{Ge}(p,t)$ and $^{70,72}\text{Ge}(t,p)$ reactions have demonstrated that the shape transition occurs between ^{72}Ge and ^{74}Ge . It has also been shown in $^{78-86}\text{Kr}(p,p')$ studies³ that the neutron number dependence on strengths of the transition to the 2_2^+ and 4_1^+ states cannot be reproduced with simple macroscopic models, implying the occurrence of the shape transition between $^{78-82}\text{Kr}$ and $^{84-86}\text{Kr}$.

The ground state band up to the 4^+ state in the $^{74-82}\text{Se}$ isotopes has been studied by Matsuki *et al.*⁴ via inelastic scattering of polarized protons at 64.8 MeV. They have pointed out that a static or dynamic hexadecapole shape transition occurs between the light $^{74,76,78}\text{Se}$ and the heavy $^{80,82}\text{Se}$ isotopes, and that the hexadecapole degree of freedom may play an important role in the structure of $^{74-82}\text{Se}$ nuclei.

Besides the behaviors of the ground state band, the low-lying states also show interesting transitional behavior. Matsuki *et al.*⁵ have found the octupole vibrational strengths splitting to two states in light $^{76-82}\text{Kr}$ isotopes. Delaroche *et al.*⁶ have reported a systematical investigation of the $^{76-82}\text{Se}(\bar{p},p')$ reactions and have also suggested that the first 3^- states of $^{76,78,80}\text{Se}$ do not have a simple vibrational character of the octupole modes.

In contrast to the strong occurrence of the octupole vibrational mode in the low-lying 3^- states, a few collective hexadecapole states have been reported; only in the even isotopes of Zn, Cd, and Pb have 4^+ states with transition strength of more than seven single-particle units (spu) been observed.⁷⁻¹⁰ No strongly collective 4^+ states have been observed in Ge, Se, or Te.^{11,12} These results may indicate that the hexadecapole vibrational strengths split into many states in these nuclei.

In view of these circumstances, high-resolution studies of low-lying excited states up to ~ 5 MeV are important.

In spite of many previous studies of Se isotopes with various reactions, no detailed high resolution studies of Se isotopes up to higher excited states have been reported yet. In the present study of $^{74-82}\text{Se}$ isotopes with the high-resolution (p,p') reaction, many levels with excitation energy up to 4.8–5.5 MeV were observed for the first time. Angular distributions obtained were analyzed with both distorted-wave Born-approximation (DWBA) and coupled-channels (CC) calculations, and spin-parity assignments are proposed to most of the levels. The present paper contains experimental data and the comparison with other experimental studies. Furthermore, the present experimental results were compared with the theoretical predictions based on the random-phase approximation (RPA) in addition to the calculation reported previously.¹³

II. EXPERIMENTAL PROCEDURE

The inelastic scattering was studied with 64.8 MeV protons from the azimuthally-varying-field (AVF) cyclotron of the Research Center for Nuclear Physics (RCNP) of Osaka University. Targets of about 0.5 mg/cm^2 in thickness were fabricated by vacuum evaporation of enriched selenium metal on thin Au backings. The enrichment was 77.71% for ^{74}Se , 96.88% for ^{76}Se , 98.58% for ^{78}Se , 99.45% for ^{80}Se , and 96.813% for ^{82}Se targets, respectively. The isotopic contents of the selenium targets are listed in Table I. The target thickness was determined by weight and checked by the comparison of elastic-scattering cross sections with the optical model prediction.

Scattered protons were momentum analyzed with the QDDQ magnetic spectrograph RAIDEN,¹⁴ and detected in the focal plane with a long multiwire proportional-counter system.¹⁵ The overall energy resolution was typically 20 keV full width at half maximum (FWHM). Data were taken in steps of 4° typically from 8° to 60° in laboratory angle.

Momentum spectra of inelastically scattered protons at $\theta_{\text{lab}} = 20^\circ$ are shown in Figs. 1–5. Yields for overlapped peaks were resolved with the method of automatic peak

TABLE I. Isotope contents of selenium targets used in the present study.

Atomic percent (%)	Target				
	⁷⁴ Se	⁷⁶ Se	⁷⁸ Se	⁸⁰ Se	⁸² Se
⁷⁴ Se	77.71	0.14	0.06	0.03	0.13
⁷⁶ Se	4.55	96.88	0.11	0.08	0.19
⁷⁷ Se	2.06	0.85	0.17	0.05	0.30
⁷⁸ Se	4.97	0.99	98.58	0.19	0.60
⁸⁰ Se	7.85	0.95	1.00	99.45	1.96
⁸² Se	2.86	0.18	0.08	0.19	96.81

fitting by a computer. By careful comparison of the peaks observed in the enriched ⁷⁴–⁸²Se and natural Se targets with each other, contaminant peaks were identified and eliminated.

Absolute cross sections were estimated to be accurate to within $\pm 10\%$. The uncertainties in the observed level energies were typically ± 2 keV below 3.0 MeV and ± 4.0 keV above 3.0 MeV in excitation energies.

III. EXPERIMENTAL RESULTS AND ANALYSES

A. Elastic-scattering data and optical-model analysis

The present elastic-scattering data were used to deduce optical-model parameters. The optical-model analysis

was made by the search code MAGALI,¹⁶ which employs an optical-model potential of the form

$$U(r) = -V_R f(r, R_R, a_R) - iW f(r, R_W, a_W) + i4a_S W_S \frac{df}{dr}(r, R_S, a_S) - \left[\frac{\hbar}{m_\pi c} \right]^2 \frac{1}{r} V_{LS} \frac{df}{dr}(r, R_{LS}, a_{LS})(\sigma \cdot L) + V_C(r, R_C),$$

where $R_X = r_X A^{1/3}$ ($X = R, W, S, LS, C$) and $f(r)$ is the standard Woods-Saxon shape function. V_C is the Coulomb potential. The calculated angular distributions of the elastic scattering divided by the Rutherford cross section $\sigma/\sigma_{\text{Ruth}}$ are shown in Fig. 6 together with the experimental data. The optical-model parameters used in this calculation are listed in Table II.

B. Inelastic-scattering data and DWBA and CC analyses

As seen in Figs. 1–5, many levels (more than 20 levels) were observed in each Se isotope in the region below about 5.0 MeV of the excitation energy. Those levels are listed in Tables III–VII. The observed angular distributions are shown in Figs. 7–11.

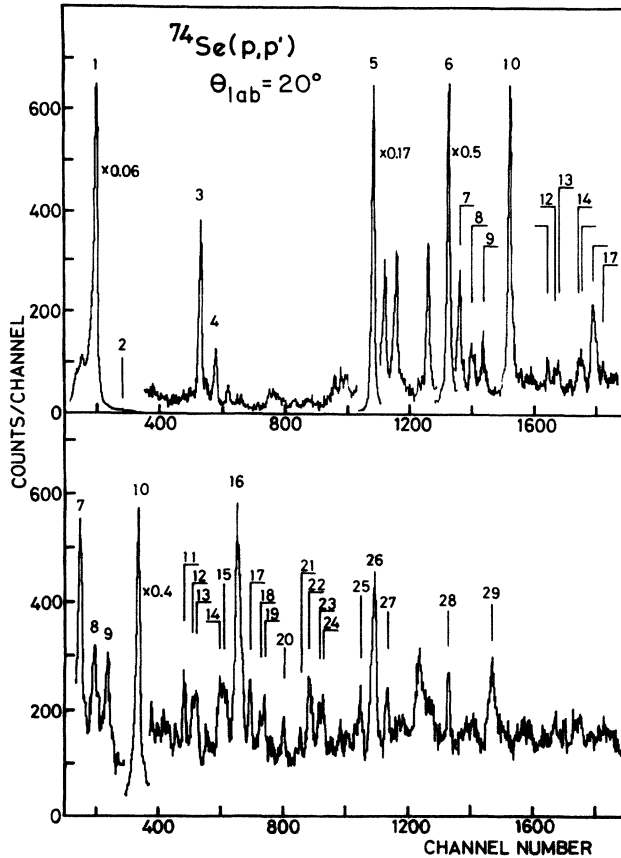


FIG. 1. Momentum spectra of protons from the ⁷⁴Se(p,p') reaction at $\theta_{\text{lab}} = 20^\circ$. Unlabeled peaks correspond to other Se isotopes in the target or impurities. The numbers on top of the peaks refer to level numbers listed in Table III.

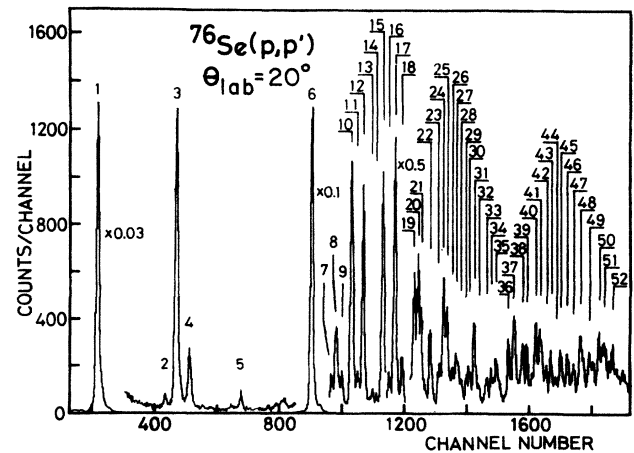


FIG. 2. Momentum spectra of protons from the ⁷⁶Se(p,p') reaction at $\theta_{\text{lab}} = 20^\circ$. The numbers on top of the peaks refer to level numbers listed in Table IV.

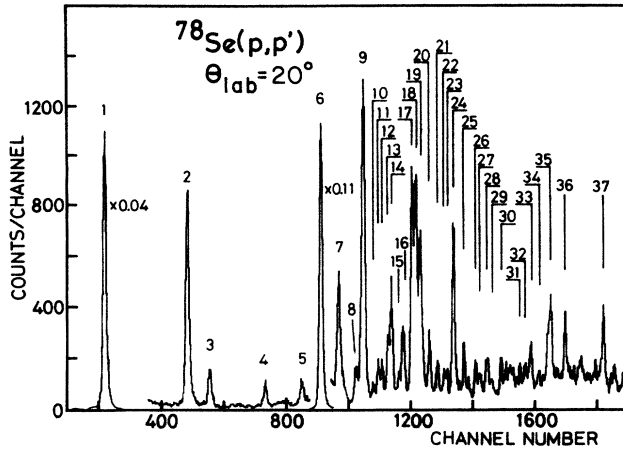


FIG. 3. Momentum spectra of protons from the $^{78}\text{Se}(p,p')$ reaction at $\theta_{\text{lab}}=20^\circ$. The numbers on top of the peaks refer to level numbers listed in Table V.

1. General description of analysis

The theoretical differential cross sections were calculated in the framework of the vibrational model with both the CC code ECIS79 (Ref. 16) and the DWBA code

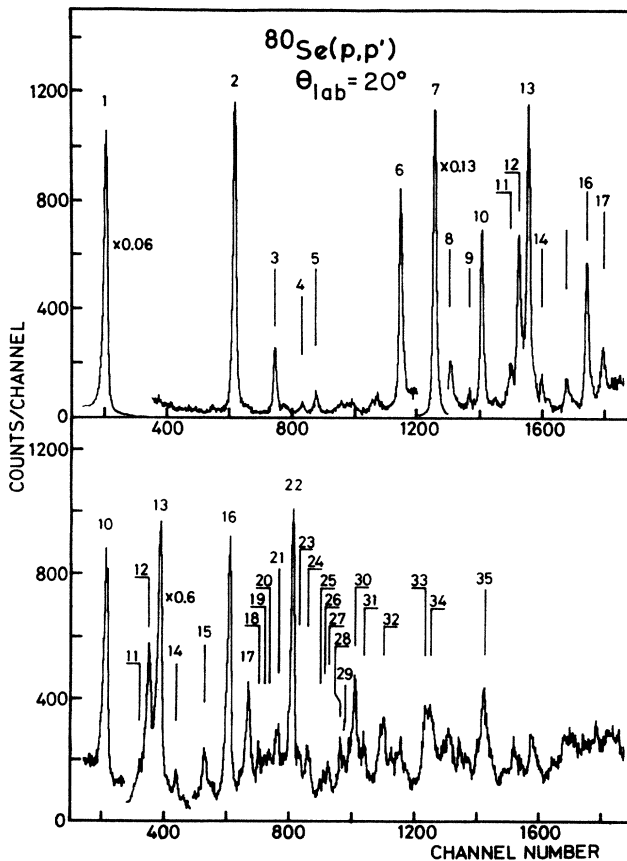


FIG. 4. Momentum spectra of protons from the $^{80}\text{Se}(p,p')$ reaction at $\theta_{\text{lab}}=20^\circ$. The numbers on top of the peaks refer to level numbers listed in Table VI.

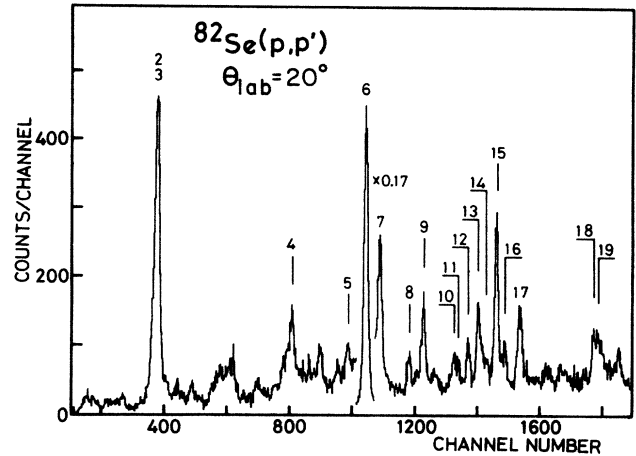


FIG. 5. Momentum spectra of protons from the $^{82}\text{Se}(p,p')$ reaction at $\theta_{\text{lab}}=20^\circ$. Unlabeled peaks correspond to other Se isotopes in the target or impurities. The numbers on top of the peaks refer to level numbers listed in Table VII.

DWUCK-4 (Ref. 17) using the standard collective-model form factors. The CC calculations for the 2_1^+ and 4_1^+ states were performed using the second-order harmonic vibrational model with $0_{g.s.}^+ - 2_1^+ - 4_1^+$ couplings. In this model, the 4_1^+ state was assumed to have mixed components of one- and two-phonon states in the form

$$|4_1^+\rangle = \cos\theta | \text{one phonon} \rangle + \sin\theta | \text{two phonon} \rangle .$$

The mixing parameter θ was chosen to give the optimum fit with the angular distribution for the 4_1^+ state and the deformation parameters β_4 were thus obtained. The CC calculations for the other states were performed using the first-order vibrational model with $0_{g.s.}^+ - 2_1^+$ and $0_{g.s.}^+ - J^\pi$ couplings, in which the same deformation parameters obtained from the second-order vibrational model were used

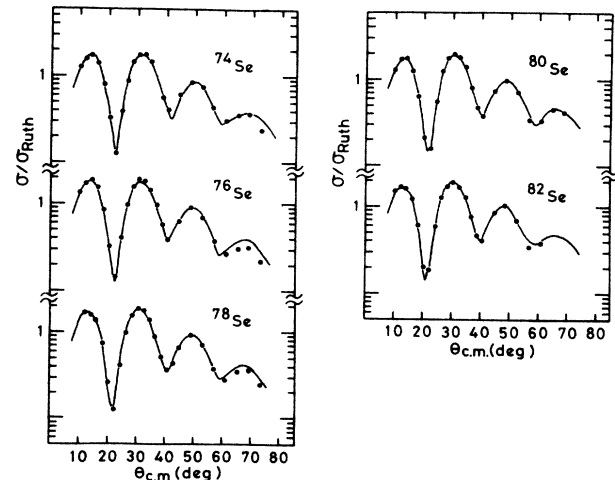


FIG. 6. Differential elastic scattering cross section (divided by the Rutherford differential scattering cross section) for 64.8 MeV protons on $^{74-82}\text{Se}$. The solid curves show the optical-model cross sections calculated with the parameters listed in Table II.

TABLE II. The best fitted optical model parameters of proton elastic scattering on $^{74-82}\text{Se}$ nuclei.

Nuclei	V_R (MeV)	r_R (fm)	a_R (fm)	W_V (MeV)	r_V (fm)	a_V (fm)	W_S (MeV)	r_S (fm)	a_S (fm)	V_{LS} (MeV)	r_{LS} (fm)	a_{LS} (fm)
^{74}Se	39.768	1.163	0.751	7.227	1.403	0.621	2.020	1.311	0.296	6.045	1.002	0.785
^{76}Se	41.324	1.156	0.752	7.091	1.379	0.624	2.542	1.390	0.310	6.039	1.019	0.791
^{78}Se	41.556	1.156	0.750	6.951	1.375	0.633	3.027	1.389	0.340	6.045	1.022	0.791
^{80}Se	41.828	1.157	0.752	6.955	1.375	0.627	3.356	1.382	0.362	6.043	1.036	0.788
^{82}Se	41.037	1.161	0.748	7.391	1.378	0.639	3.289	1.358	0.411	6.076	1.040	0.741

for the 2_1^+ states and other states were assumed to be the natural parity states. The present results of the J^π values thus obtained are summarized in Tables III–VII. The deformation parameters for the 2^+ , 3^- , and 4^+ states were deduced in terms of $\beta_L R$ values from the CC calculations by using a relation $R = r_0 A^{1/3}$ where a real-well radius was assumed to be $r_0 = 1.22$ fm. Those values are listed in Tables VIII–X, and errors are estimated to be less than $\pm 10\%$.

The energy weighted sum-rule (EWSR) fraction (ΔS) for the observed states were calculated from the formula

$$\Delta S = \frac{3}{2\pi} \frac{E_x (\beta_L R)^2}{L(2L+1)^2} \frac{mc^2}{(\hbar c)^2},$$

where E_x is the excitation energy. These ΔS values for the 2^+ , 3^- , and 4^+ states are also listed in Table VIII–X.

2. The 2_1^+ , 4_1^+ , 2_2^+ , and 0_2^+ states

The angular distributions for the 2_1^+ states have similar shape in all isotopes, and are better described with the CC calculations than the DWBA as seen in Figs. 7–11. The

TABLE III. Levels populated in the present $^{74}\text{Se}(p,p')$ reaction and comparison to the other data.

No.	Present			Previous ^a	
	E_x (MeV)	L	J^π	E_x (MeV)	J^π
1	0.635	2	2^+	0.6348	2^+
2	0.856	0	0^+	0.8538	0^+
3	1.268	2	2^+	1.2689	2^+
4	1.363	4	4^+	1.3632	4^+
5	2.350	3	3^-	2.3497	3^-
6	2.844	3	3^-	2.8318	
7	2.903	4	4^+	2.9188	
8	3.002				
9	3.080	4	4^+	3.0782	
10	3.259	4	4^+	3.2500	
11	3.529	5	5^-	3.5396	
12	3.579	2	2^+	3.5803	
13	3.602	5	5^-		
14	3.749	4	4^+	3.749	(5^-)
15	3.780	4	4^+	3.7882	(1^-)
16	3.845	3	3^-	3.847	(7^-)
17	3.920				
18	3.980	(6)	(6^+)	3.9729	
19	4.005	(2)	(2^+)	4.000	
20	4.118			4.100	
21	4.224				
22	4.279	4	4^+	4.2667	(1^-)
				4.290	
23	4.337	(2)	(2^+)	4.3425	
24	4.362			4.3799	(1^-)
				4.5863	
25	4.595	4	4^+	4.5930	$(-)$
26	4.677	3	3^-	4.6617	
27	4.758	(3)	(3^-)	4.7572	
28	5.146	3	3^-		
29	5.426	3	3^-		

^aReference 18.

TABLE IV. Levels populated in the present $^{76}\text{Se}(p,p')$ reaction and comparison to the other data.

No.	Present			Previous ^a	
	E_x (MeV)	L	J^π	E_x (MeV)	J^π
1	0.559	2	2 ⁺	0.5591	2 ⁺
2	1.122	0	0 ⁺	1.1224	0 ⁺
3	1.216	2	2 ⁺	1.2161	2 ⁺
4	1.330	4	4 ⁺	1.3308	4 ⁺
5	1.787	2	2 ⁺	1.7877	2 ⁺
6	2.429	3	3 ⁻	2.4288	3 ⁻
				2.616	
7	2.621	4	4 ⁺	2.628	
8	2.658			2.6555	(1)
9	2.691	(3)	(3 ⁻)	2.6698	(2)
10	2.807	4	4 ⁺	2.805	
11	2.853	4	4 ⁺	2.862	
12	2.915	4	4 ⁺	2.923	
13	3.001	2	2 ⁺	3.010	
				3.022	
14	3.042	6	6 ⁺		
15	3.103	3	3 ⁻	3.1065	
16	3.160	3	3 ⁻	3.1601	
17	3.216	3 + 4	3 ⁻ + 4 ⁺	3.212	
18	3.289	4	4 ⁺	3.268	(3 ⁻ , 4 ⁻)
19	3.408	4	4 ⁺	3.417	
20	3.443	3	3 ⁻	3.442	
21	3.475	4	4 ⁺	3.4652	
22	3.565			3.5565	
23	3.655	(3)	(3 ⁻)		
24	3.697			3.700	
25	3.732	3	3 ⁻	3.741	
26	3.776	4	4 ⁺	3.790	
27	3.806	5	5 ⁻	3.808	
28	3.862	4	4 ⁺	3.856	
29	3.917	4	4 ⁺		
30	3.948	4	4 ⁺	3.955	
31	3.999	3	3 ⁻	3.999	
32	4.042				
33	4.119			4.103	
				4.133	
34	4.170	4	4 ⁺	4.173	
35	4.218	3	3 ⁻	4.216	
36	4.340	3	3 ⁻	4.343	
37	4.399	4	4 ⁺	4.400	
38	4.476	(2)	(2 ⁺)	4.475	
39	4.523	3	3 ⁻	4.527	
40	4.611	3	3 ⁻	4.604	
41	4.658	3	3 ⁻	4.647	
				4.677	
42	4.723	4	4 ⁺	4.729	
43	4.771	(3)	(3 ⁻)	4.755	
44	4.811				
45	4.859	4	4 ⁺	4.858	
46	4.935	3	3 ⁻	4.938	
47	4.998			5.013	
48	5.081	3	3 ⁻	5.091	
49	5.174	3	3 ⁻		
50	5.261	4	4 ⁺		
51	5.303	3	3 ⁻		
52	5.401				

^aReference 19.

TABLE V. Levels populated in the present $^{78}\text{Se}(p,p')$ reaction and comparison to the other data.

No.	Present			Previous ^a	
	E_x (MeV)	L	J^π	E_x (MeV)	J^π
1	0.614	2	2 ⁺	0.6138	2 ⁺
2	1.308	2	2 ⁺	1.3086	2 ⁺
3	1.503	4	4 ⁺	1.5026	4 ⁺
4	1.993	2	2 ⁺	1.9960	(2 ⁺)
5	2.330	2	2 ⁺	2.3273	(2 ⁺)
				2.3347	(0,1,2)
6	2.508	3	3 ⁻	2.5076	3 ⁻
7	2.678	4	4 ⁺	2.6801	
				2.6821	(1 ⁻ ,2,3 ⁻)
8	2.840			2.8386	(1,2 ⁺)
				2.8984	(1,2 ⁺)
9	2.906	4	4 ⁺	2.9145	
10	3.003			3.0052	(1,2 ⁺)
11	3.049	(3)	(3 ⁻)	3.0484	
12	3.085	5	5 ⁻	3.0903	(0) ⁺
13	3.140	4	4 ⁺	3.1396	≤ 4
14	3.176			3.1819	(1,2) ⁺
				3.2429	(1,2 ⁺)
15	3.249	2	2 ⁺	3.2551	(1,2 ⁺)
16	3.288	4	4 ⁺	3.2884	(0,1,2)
17	3.376	3	3 ⁻	3.3727	(1,2,3)
18	3.414	3	3 ⁻	3.4114	(1 ⁻ ,2,3)
19	3.453	3	3 ⁻	3.4477	
20	3.546			3.5225	(2,3) ⁺
21	3.605	2	2 ⁺	3.5926	(0,1,2)
				3.6038	≤ 4
22	3.683			3.6857	(1,2,3) ⁻
23	3.710			3.7114	(1,2,3)
24	3.774	3	3 ⁻		
25	3.881	3	3 ⁻		
26	3.995	5	5 ⁻	3.9992	(0,1,2)
27	4.050	(5)	(5 ⁻)	4.0365	
28	4.120	4	4 ⁺		
29	4.157	3	3 ⁻	4.1523	(0,1) ⁻
30	4.254	(4)	(4 ⁺)		
31	4.424	(2)	(2 ⁺)		
32	4.493	(3)	(3 ⁻)	4.490	(1,2,3) ⁻
33	4.557				
34	4.622	5	5 ⁻		
35	4.741	4	4 ⁺		
36	4.902	3	3 ⁻	4.910	(1,2,3) ⁻
37	5.296	3	3 ⁻		

^aReference 20.

4_1^+ and 2_2^+ states in ^{82}Se were not resolved in this experiment, because the excitation energies for these states are very close. The angular distributions for these states in ^{82}Se were assumed to be of the same shape as those of the corresponding states in ^{80}Se , and the absolute values for these states were obtained so as to reproduce the unresolved and summed angular distributions by a linear combination of the two assumed cross sections for the 4_1^+ and 2_2^+ states with a χ^2 -fitting criterion. The angular distributions for the 4_1^+ and 2_2^+ states resolved with this method are shown in Fig. 11. A similar procedure was also applied to the unresolved 4_1^+ and 0_2^+ states in ^{78}Se .

The cross sections for this 4_1^+ state are about ten times larger than those for the 0_2^+ state at all angles measured.

The second-order vibrational model with $0_{g.s.}^+ - 2_1^+ - 4_1^+$ couplings was used to calculate the angular distributions for the 2_1^+ and 4_1^+ states, and the results are shown in Figs. 7–11. The angular distributions for the 2_2^+ states are also shown and are well described with the CC predictions using the first-order vibrational model.

As shown in Fig. 2, the cross sections are in the order of $\sigma(2_2^+) > \sigma(4_1^+) \gg \sigma(0_2^+)$. The 0_2^+ states were only weakly observed in $^{74,76}\text{Se}$ and not observed in $^{80,82}\text{Se}$: At around $\theta_{c.m.} \sim 30^\circ$, the cross sections for the 0_2^+ states are

TABLE VI. Levels populated in the present ⁸⁰Se(p,p') reaction and comparison to the other data.

No.	Present			Previous ^a	
	E_x (MeV)	L	J^π	E_x (MeV)	J^π
1	0.666	2	2 ⁺	0.6662	2 ⁺
2	1.449	2	2 ⁺	1.4493	2 ⁺
				1.4791	0 ⁺
3	1.701	4	4 ⁺	1.7015	4 ⁺
4	1.871	2	2 ⁺	1.8734	0,2 ⁺
5	1.960	2	2 ⁺	1.9602	2 ⁽⁺⁾
6	2.497	4	4 ⁺	2.4953	(2,3,4)
				2.5147	2 ⁽⁺⁾
7	2.718	3	3 ⁻	3.7174	3 ⁻
8	2.819	(2)	(2 ⁺)	2.8142	2 ⁽⁺⁾
9	2.946	(2)	(2 ⁺)	2.9475	(\leq 4)
10	3.033	4	4 ⁺	3.0250	(1,2 ⁺)
11	3.226	4	4 ⁺	3.2266	(1,2)
12	3.284	3	3 ⁻	3.2804	(1,2 ⁺)
13	3.354	3	3 ⁻	3.3504	(1 ⁺)
14	3.445	2	2 ⁺	3.4414	(0 ⁺)
				3.6065	(2 ⁺)
15	3.619	(2)	(2 ⁺)	3.6197	(0 ⁺)
16	3.753	3	3 ⁻	3.754	
17	3.868			3.8703	(1,2)
18	3.931	(2)	(2 ⁺)	3.9305	
19	3.960	(2)	(2 ⁺)	3.9520	(1,2)
				3.965	
20	3.996	5	5 ⁻	4.011	
				4.023	
21	4.039			4.0471	(\leq 4)
22	4.130	3	3 ⁻	4.125	
23	4.173	(2)	(2 ⁺)	4.169	
24	4.225			4.233	
25	4.295			4.303	
26	4.322			4.333	
27	4.352				
28	4.420	(2)	(2 ⁺)		
29	4.442	5	5 ⁻		
30	4.511	4	4 ⁺		
31	4.570				
32	4.682	4	4 ⁺		
33	4.950				
34	4.993				
35	5.325	3	3 ⁻		

^aReference 21.

$\sim 70 \mu\text{b/sr}$ for ⁷⁴Se, $\sim 200 \mu\text{b/sr}$ for ⁷⁶Se, and less than $20 \mu\text{b/sr}$ for ^{80,82}Se, respectively. The feature of the most prominent excitation for the 0_2^+ state in ⁷⁶Se is consistent with the result by Delaroche *et al.*⁶

C. ⁷⁴Se(p,p') reaction

Twenty-nine levels of ⁷⁴Se were populated up to 5.5 MeV excitation energy. The measured angular distributions are shown in Fig. 7. The results are summarized in Table III together with the known data for energy, spin, and parity obtained from Ref. 18. In the present experiment, there were several contaminant peaks due to the

poor enrichment (77.71%) of the ⁷⁴Se target. A careful comparison between the spectra of the ⁷⁴Se target and those of other Se targets (enriched ⁷⁶⁻⁸²Se and natural Se) allowed us to eliminate such contaminant peaks.

$L \leq 2$ transition: The angular distributions of 0.635 MeV (2_1^+) and 1.268 MeV (2_2^+) states are well reproduced with the CC calculations as shown in Fig. 7. A tentative assignment of $J^\pi = 2^+$ was obtained for the 3.579 MeV level.

$L = 3$ transition: The lowest 3^- level at 2.350 MeV was strongly excited. The measured excitation energy was in good agreement with those of previous studies. Five levels above 2.5 MeV excitation energy were observed

TABLE VII. Levels populated in the present $^{82}\text{Se}(p,p')$ reaction and comparison to the other data.

No.	Present			Previous ^a	
	E_x (MeV)	L	J^π	E_x (MeV)	J^π
1	0.654	2	2^+	0.656 1.414	2^+ (0^+)
2	1.731	2	2^+		
3	1.734	4	4^+	1.753	$2^+, 4^+$
4	2.552			2.546	
5	2.899	5	5^-	2.897	
6	3.015	3	3^-	3.012	3^-
7	3.106	4	4^+	3.101	(5^-)
8	3.293	4	4^+		
9	3.384	3	3^-		
10	3.587	2	2^+	3.581	2^+
11	3.624				
12	3.677	4	4^+	3.669	2^+
13	3.750	2	2^+	3.748	2^+
14	3.798	4	4^+		
15	3.866	3	3^-	3.834	0^+
16	3.916	2^+	2^+	3.921	2^+
17	4.026			4.010 4.134 4.396 4.466	2^+ 2^+ 2^+ (4^+)
18	4.538			4.518	(4^+)
19	4.586	4	4^+	4.578 4.809 4.969 5.029	(4^+) (1^-) (1^-) (1^-)

^aReference 22.

with $L=3$ transitions and proposed to be $J^\pi=3^-$.

$L=4$ transition: The previously known 4_1^+ level at 1.363 MeV was weakly observed. The angular distribution of this state was not reproduced by the one-step DWBA calculation with the $L=4$ transition, but was well described by the CC prediction with a positive deformation parameter β_4 as shown in Fig. 7. Seven levels observed above 2.5 MeV excitation energy have a shape with the $L=4$ transition and their spins are proposed to be $J^\pi=4^+$ as shown in the figure.

Other transitions: Two levels with $L=5$ transitions were identified at 3.529 and 3.602 MeV and assigned as $J^\pi=5^-$.

D. $^{76}\text{Se}(p,p')$ reaction

Fifty-two levels in ^{76}Se were populated up to 5.5 MeV excitation energy. The measured angular distributions are shown in Fig. 8. The results are summarized in Table IV together with the previously known data obtained from Ref. 19. Below 2.5 MeV, the present results for excitation energies are in excellent agreement with those of the previously known states.

$L \leq 2$ transition: The known levels at 0.559, 1.216, and 1.787 MeV with $J^\pi=2^+$ were also observed in this experiment. The 3.001 MeV level showed that the angular distribution was similar to those $L=2$ transitions for the

1.216 and 1.787 MeV states, and was proposed to be $J^\pi=2^+$. The 0_2^+ level was weakly excited at 1.122 MeV.

$L=3$ transitions: The first 3^- level in ^{76}Se was strongly excited. Fourteen levels with $L=3$ transitions were observed above 3.0 MeV excitation energy and then assigned as $J^\pi=3^-$.

$L=4$ transitions: The first 4^+ level which was known in previous studies was observed at 1.330 MeV. Sixteen levels observed above 2.5 MeV excitation energy have angular shapes with $L=4$ transitions and are proposed as $J^\pi=4^+$. The angular distribution for the 4_1^+ state was well reproduced using the CC calculation with a positive deformation parameter β_4 .

Other transitions: The angular distribution for the 3.216 MeV level was excited strongly, and found to be a doublet with $L=3$ and 4 transitions. Each angular distribution for these two levels was obtained by fitting the unresolved angular distributions to a linear sum of the known cross sections for the 3^- ($E_x=3.103$ MeV) and 4^+ ($E_x=2.807$ MeV) levels in ^{76}Se , and both the deformation parameters were obtained. The same methods to reproduce the summed cross section with other combinations of the L transitions were done, but no good fit was obtained. A level at 3.806 MeV has a shape of $L=5$ transitions and proposed to be $J^\pi=5^-$. The transition of $L=6$ was also observed at 3.042 MeV and $J^\pi=6^+$ was proposed for this level.

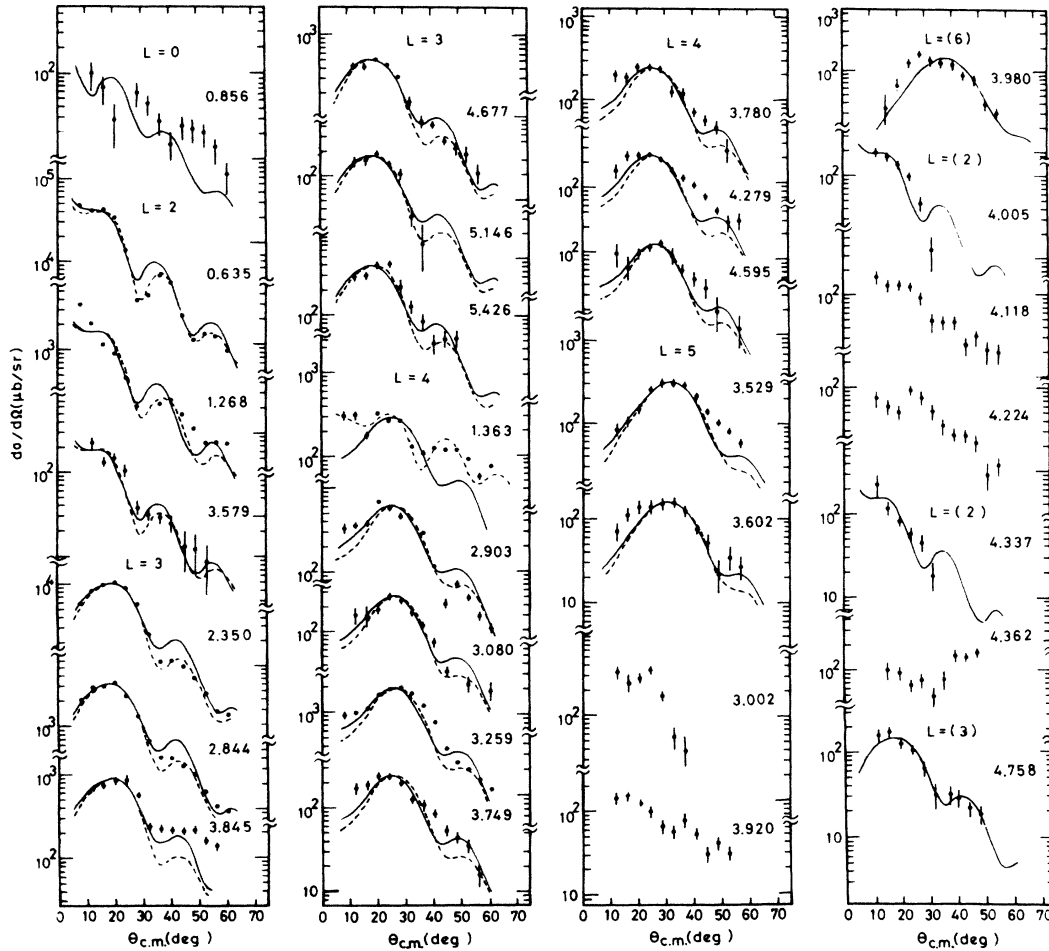


FIG. 7. Angular distributions of protons from the $^{74}\text{Se}(p,p')$ reaction. Vertical bars represent statistical errors only. The solid and dashed lines are the predictions of the DWBA and CC analyses, respectively, using the optical-model parameters listed in Table II. The relevant states calculated with the CC analysis are used in $0_{g.s.}^+ - 2_1^+ - j^\pi$ coupling with the second-order vibrational model for the 2_1^+ and 4_1^+ states, and with the first-order vibrational model for the other states.

E. $^{76}\text{Se}(p,p')$ reaction

Thirty-seven levels were populated up to 5.4 MeV excitation energy. The measured angular distributions are shown in Fig. 9. The results are summarized in Table V, together with the known data for energy, spin, and parity cited from Ref. 20.

$L \leq 2$ transitions: The 2^+ levels at 0.614 and 1.308 MeV were observed and the excitation energies were in good agreement with previous studies. Weak $L=2$ transitions were seen at 1.993, 2.330, 3.249, and 3.605 MeV and these levels were proposed as $J^\pi = 2^+$.

$L=3$ transitions: The first 3^- at 2.508 MeV was strongly excited and this excitation energy was in good agreement with the previous result. Eight levels with the $L=3$ transition was observed above 3.0 MeV excitation energy and proposed as $J^\pi = 3^-$.

$L=4$ transitions: The first 4^+ level was observed at 1.503 MeV. Six levels observed above 2.5 MeV excitation energy have a shape with the $L=4$ transition and are proposed as $J^\pi = 4^+$. The angular distribution for the 4_1^+

level was well reproduced using the CC calculation with a small deformation parameter β_4 .

Other transitions: The 3.085, 3.995, and 4.622 MeV levels were weakly excited with $L=5$ transitions.

F. $^{80}\text{Se}(p,p')$ reaction

Thirty-five levels in ^{80}Se were populated up to 5.5 MeV excitation energy. The measured angular distributions are shown in Fig. 10. The results are summarized in Table VI together with the previously known data for energy, spin, and parity cited from Ref. 21.

$L \leq 2$ transitions: The 2^+ levels were observed at 0.666 and 1.449 MeV with $L=2$ transitions in good agreement with the previous data. Other $L=2$ transitions were also observed at 1.871, 1.960, and 3.445 MeV. These levels were also proposed as $J^\pi = 2^+$.

$L=3$ transitions: The known first 3^- level at 2.718 MeV was strongly excited. Other previously unknown $L=3$ transitions were also found at 3.284, 3.354, 3.753, 4.130, and 5.325 MeV and proposed as $J^\pi = 3^-$.

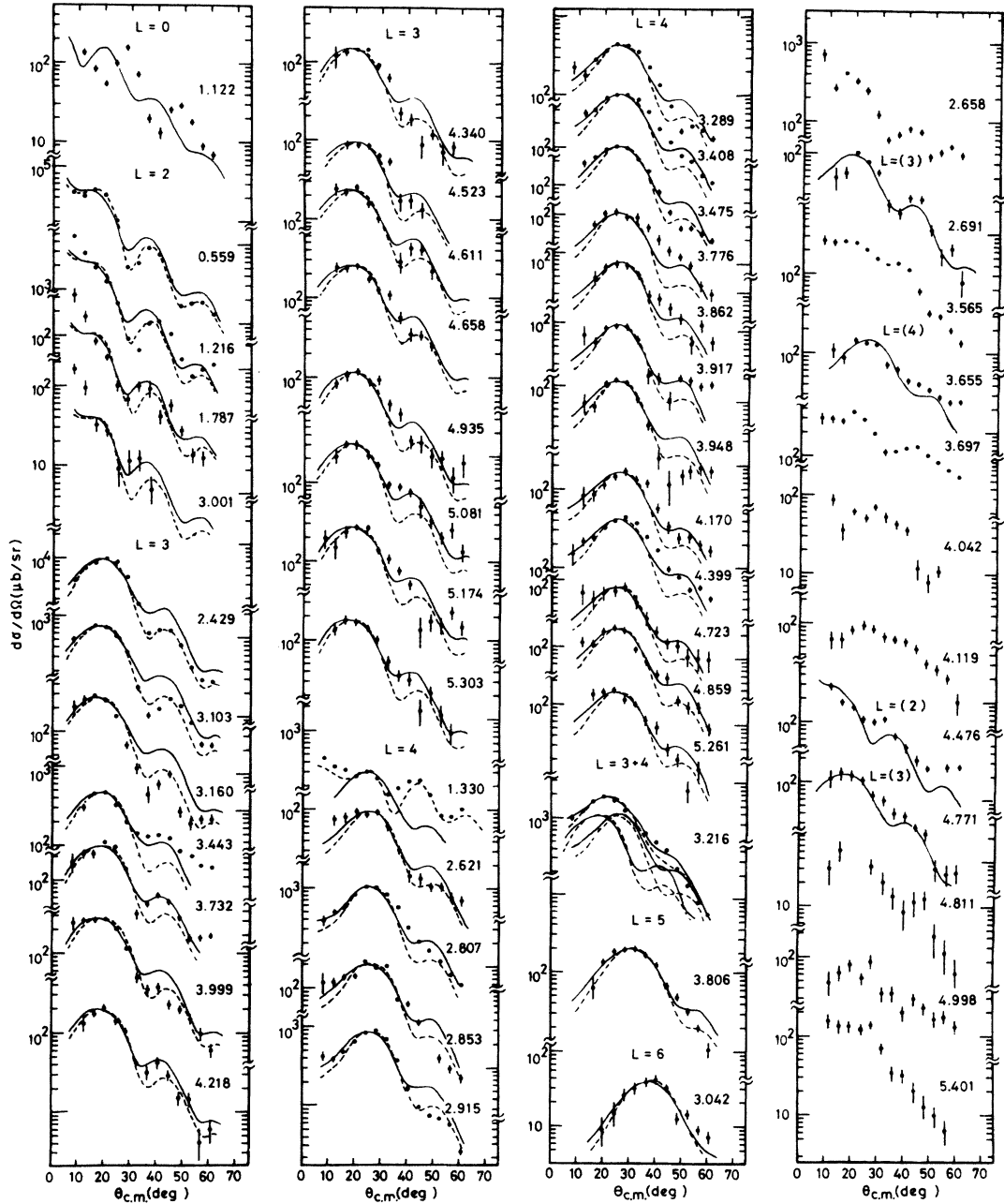


FIG. 8. Angular distributions of protons from the $^{76}\text{Se}(p,p')$ reaction. See also the caption for Fig. 7.

L = 4 transitions: The known first 4^+ level at 1.701 MeV was observed. Other $L = 4$ transitions were also found at 2.497, 3.033, 3.226, 4.511, and 4.682 MeV and proposed as $J^\pi = 4^+$. These levels were previously unknown. The shape of the angular distribution of the 4_1^+ level was well reproduced by the CC calculation with a negative deformation β_4 .

Other transitions: Two levels at 3.996 and 4.442 MeV were weakly populated with $L = 5$ transitions and proposed as $J^\pi = 5^-$.

G. $^{82}\text{Se}(p,p')$ reaction

Twenty levels in ^{82}Se were populated up to 4.8 MeV excitation energy. Except for the first 2^+ and 3^- levels, these levels were weakly excited. The measured angular distributions are shown in Fig. 11. The results are summarized in Table VII together with the previously known data for energy, spin, and parity obtained from the $^{80}\text{Se}(t,p)^{82}\text{Se}$ reaction study.²²

L ≤ 2 transitions: The 0.654 MeV 2_1^+ level was strongly

TABLE VIII. The excitation energies, βR values, and EWSR fractions of the quadrupole states in $^{74-82}\text{Se}$ observed in the present experiments.

E_x (MeV)	^{74}Se			^{76}Se			^{78}Se			^{80}Se			^{82}Se		
	βR	E_x (MeV)	EWSR (%)	βR	E_x (MeV)	EWSR (%)	βR	E_x (MeV)	EWSR (%)	βR	E_x (MeV)	EWSR (%)	βR	E_x (MeV)	EWSR (%)
0.635	1.38	0.559	10.64 ^a	1.45	0.614	10.70 ^a	1.33	0.666	10.16 ^a	1.03	0.654	6.75 ^a	0.86	0.654	4.78 ^a
1.268	0.23	1.216	0.58	0.26	1.308	0.76	0.23	1.449	0.62	0.25	1.731	0.89	0.21	1.731	0.74
3.579	0.08	1.787	0.18	0.06	1.993	0.07	0.07	1.871	0.08	0.05	3.587	0.05	0.10	3.587	0.31
		3.001		0.04	2.330	0.01	0.06	1.960	0.07	0.05	3.750	0.05	0.12	3.750	0.50
					3.249		0.06	3.445	0.13	0.09	3.916	0.25	0.11	3.916	0.46
					3.605		0.09		0.25						
total			11.40%			11.54%			11.31%			7.99%			6.79%

^aObtained with the CC predictions by using the second-order vibrational model.

TABLE IX. The excitation energies, βR values, and EWSR fractions of the octupole states for $^{74-82}\text{Se}$ observed in the present experiments.

E_x (MeV)	^{74}Se			^{76}Se			^{78}Se			^{80}Se			^{82}Se		
	βR	E_x (MeV)	EWSR (%)	βR	E_x (MeV)	EWSR (%)	βR	E_x (MeV)	EWSR (%)	βR	E_x (MeV)	EWSR (%)	βR	E_x (MeV)	EWSR (%)
2.350	0.77	2.429	5.83	0.69	2.508	4.95	0.70	2.718	5.39	0.66	3.015	5.44	0.68	3.015	6.45
2.844	0.43	3.103	2.19	0.19	3.376	0.49	0.19	3.284	0.55	0.20	3.383	0.59	0.12	3.383	0.22
3.845	0.22	3.160	0.77	0.11	3.414	0.18	0.20	3.354	0.58	0.25	3.866	0.99	0.19	3.866	0.66
4.677	0.17	3.216	0.58	0.23	3.453	0.73	0.18	3.753	0.47	0.16		0.46			
5.146	0.10	3.443	0.22	0.15	3.774	0.33	0.16	4.130	0.44	0.16		0.50			
5.426	0.16	3.732	0.58	0.12	3.881	0.23	0.09	5.325	0.15	0.11		0.29			
		3.999		0.11	4.157	0.23	0.06		0.08						
		4.218		0.10	4.902	0.17	0.10		0.23						
		4.340		0.09	5.296	0.13	0.12		0.31						
		4.523		0.07		0.09									
		4.611		0.11		0.24									
		4.658		0.11		0.26									
		4.935		0.07		0.11									
		5.081		0.12		0.33									
		5.174		0.12		0.31									
		5.303		0.09		0.19									
total			10.17%			8.97%			8.20%			8.27%			7.33%

TABLE X. The excitation energies, βR values, and EWSR fraction of the hexadecapole states for $^{74-82}\text{Se}$ observed in the present experiments.

E_x (MeV)	^{74}Se			^{76}Se			^{78}Se			^{80}Se			^{82}Se		
	βR	E_x (MeV)	EWSR (%)	βR	E_x (MeV)	EWSR (%)	βR	E_x (MeV)	EWSR (%)	βR	E_x (MeV)	EWSR (%)	βR	E_x (MeV)	EWSR (%)
1.363	0.09	1.330	0.05 ^a	0.06	1.503	0.01 ^a	0.00	1.701	0.00 ^a	-0.18	1.734	0.14 ^a	-0.27	1.734	0.33 ^a
2.903	0.23	2.621	0.38	0.09	2.678	0.05	0.18	2.497	0.23	0.25	3.106	0.43	0.20	3.106	0.32
3.080	0.14	2.807	0.15	0.28	2.906	0.56	0.33	3.033	0.81	0.22	3.293	0.38	0.10	3.293	0.08
3.259	0.42	2.853	1.38	0.12	3.140	0.10	0.12	3.226	0.12	0.11	3.677	0.11	0.14	3.677	0.20
3.749	0.11	2.915	0.11	0.26	3.288	0.49	0.14	4.511	0.16	0.10	3.798	0.13	0.10	3.798	0.10
3.780	0.15	3.216	0.20	0.29	4.120	0.68	0.09	4.682	0.08	0.13	4.586	0.19	0.14	4.586	0.24
4.279	0.14	3.289	0.21	0.18	4.741	0.28	0.17		0.35						
4.595	0.10	3.408	0.11	0.19	3.408	0.31									
		3.475		0.16	3.475	0.23									
		3.776		0.06	3.776	0.04									
		3.862		0.07	3.862	0.05									
		3.917		0.08	3.917	0.07									
		3.948		0.09	3.948	0.09									
		4.170		0.11	4.170	0.14									
		4.399		0.18	4.399	0.38									
		4.723		0.08	4.723	0.07									
		4.859		0.05	4.859	0.03									
		5.261		0.11	5.261	0.14									
total			2.59%			3.72%			1.75%			1.38%			1.27%

^aObtained with the CC predictions by using the second-order vibrational model.

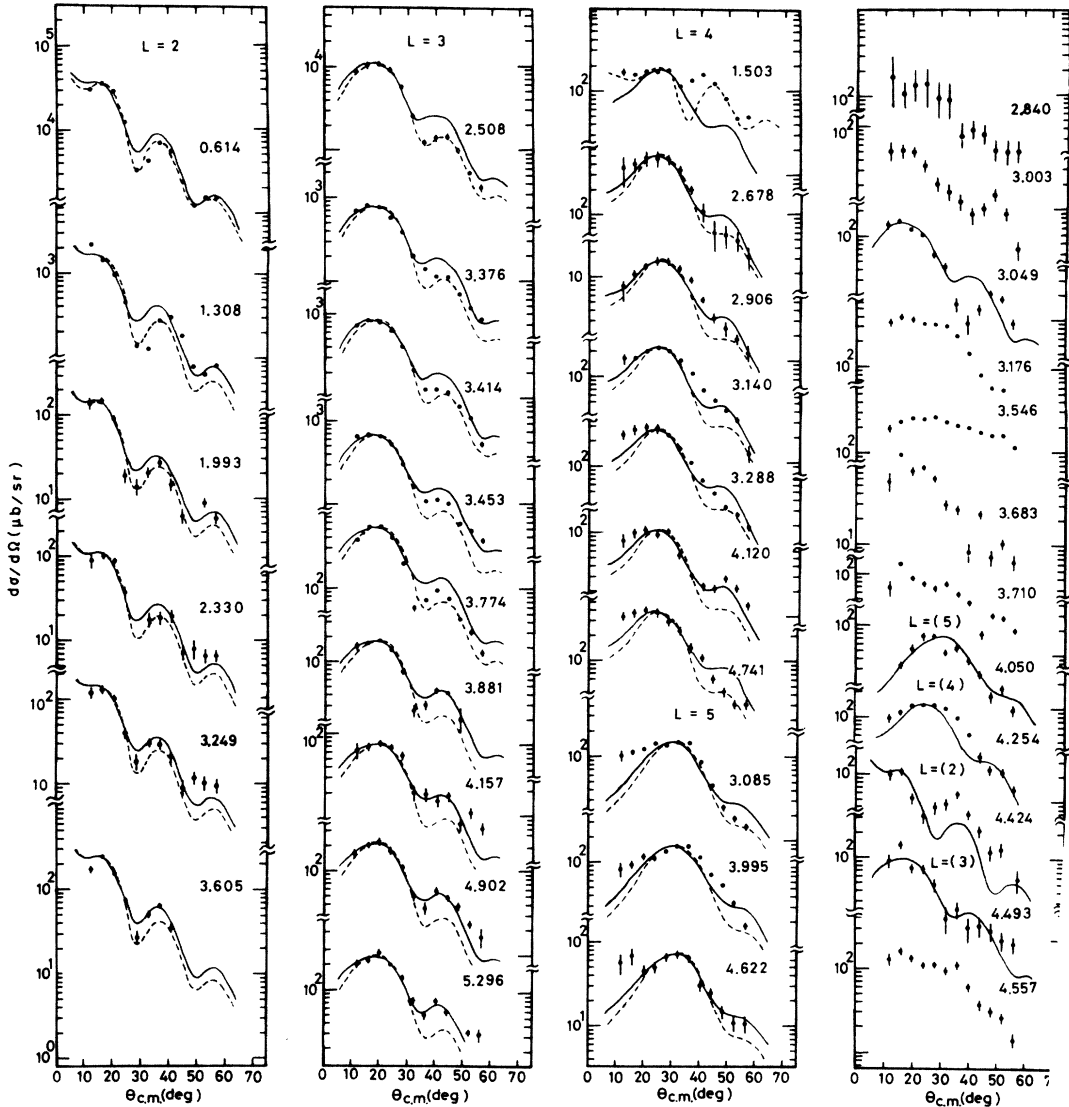


FIG. 9. Angular distributions of protons from the $^{78}\text{Se}(p,p')$ reaction. See also the caption for Fig. 7.

excited. Other $L=2$ transitions were observed at 1.731, 3.587, 3.750, and 3.916 MeV and proposed as $J^\pi=2^+$.

$L=3$ transitions: The first 3^- level at 3.015 MeV was strongly excited. Two levels at 3.384 and 3.866 MeV were observed with $L=3$ transitions and proposed as $J^\pi=3^-$.

$L=4$ transitions: Five levels at 3.106, 3.293, 3.677, 3.798, and 4.586 MeV were populated with $L=4$ transitions and proposed as $J^\pi=4^+$.

Other transitions: The 2.899 MeV level was well reproduced with $L=5$ transition and proposed as $J^\pi=5^-$.

IV. DISCUSSION

A. The energy levels and transition strengths

1. General

Many levels (more than 30 levels) were populated in the low energy region of $^{76,78,80}\text{Se}$, while in $^{74,82}\text{Se}$ fewer levels

(20–30 levels) were observed. The 2_1^+ and 3_1^- states were observed with large strengths in all Se isotopes. Several 4^+ states with comparable strengths (less than 3.0 spu) were observed in the $E_x=2.0$ –5.0 MeV region. Besides the 2_1^+ states, only a few 2^+ states were excited weakly. This feature means that only the 2_1^+ state has large collectivity, in marked contrast with the fragmentations of the transition strengths into many states in the case of $L=4$ ($J^\pi=4^+$).

^{74}Se : There have been many experimental studies^{18,23–26} of ^{74}Se with β decay, in-beam β - γ spectroscopies, Coulomb excitation, and (p,t) reactions, whereas the works on inelastic scattering studies have been rare. As seen in Table III, many states with excitation energy higher than 2.5 MeV are newly observed in the present experiment. The 3^- (4^+) level observed at 2.844 (3.259) MeV in our experiment may correspond to those observed at 2.84 (3.253) and 2.856 (3.262) MeV, respectively, in the (p,t) reactions.^{25,26}

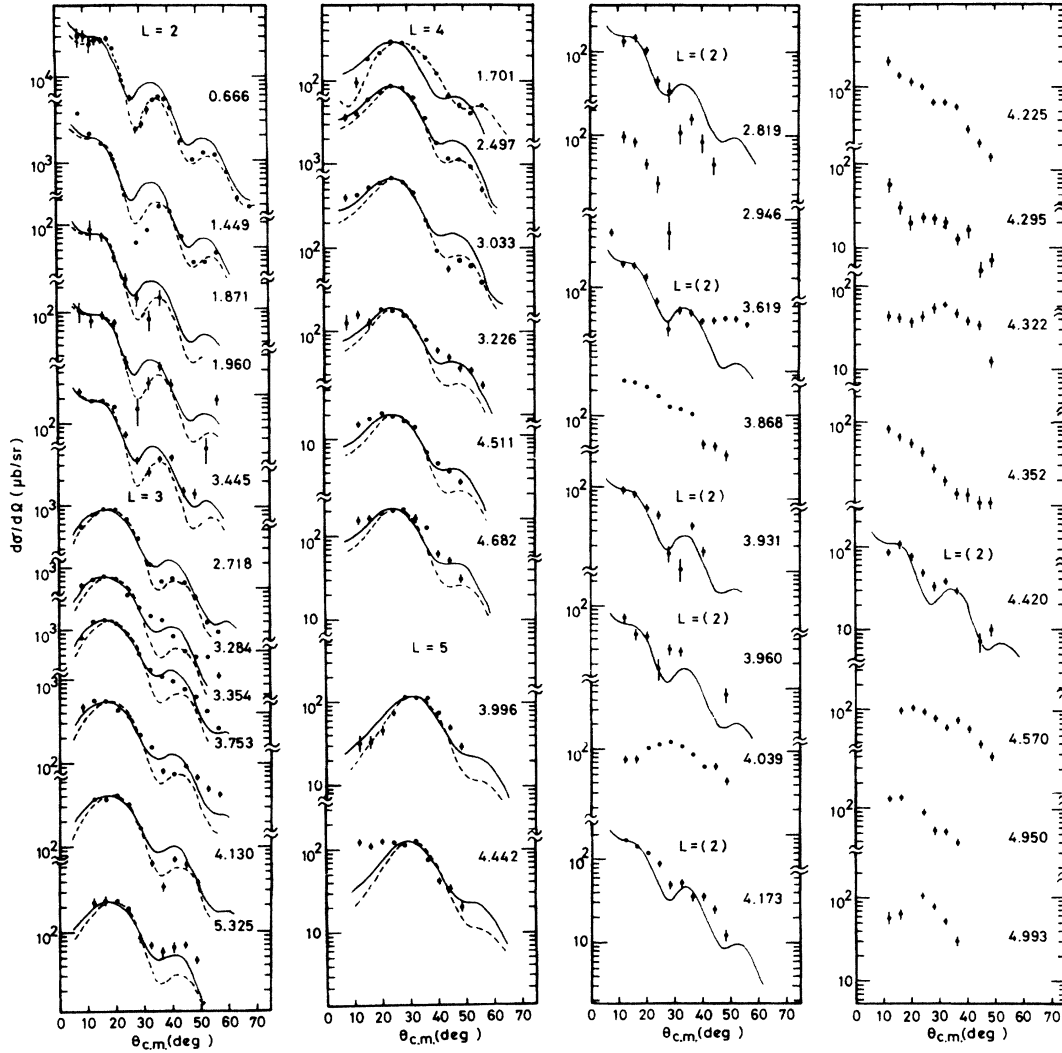


FIG. 10. Angular distributions of protons from the $^{80}\text{Se}(p,p')$ reaction. See also the caption for Fig. 7.

^{76}Se : The lower levels of ^{76}Se were previously studied^{19,27,28} via inelastic scattering, β decays, and Coulomb excitations.²⁸ Recently, in-beam spectroscopic studies of ^{76}Se were performed with the $(\alpha,2n)$,²⁹ $(\text{Li},2n)$,³⁰ and (n,γ) (Ref. 31) reactions. The observed levels with these studies are different from the results of the present study except for lower excitation levels. Tentative assignments of $J^\pi=3^-$ or 4^+ were reported to the states of 2.614, 3.232, 3.458, 3.693, and 3.980 MeV from the (p,t) study by Borsaru *et al.*²⁶ These levels may correspond to the states at 2.621 (4^+), 3.216 (3^-+4^+), 3.443 (3^-), 3.697 (3^-), and 3.999 (3^-) MeV, respectively, in the present study.

^{78}Se : There have been several studies²⁰ reported for the ^{78}Se with the (p,p') and (d,d') reactions. Hinrichsen *et al.*³² studied ^{78}Se by the $^{78}\text{Se}(p,p')$ reaction at 10 MeV with the best energy resolution of about 17 keV. They tentatively assigned $J=(1,2,3)$ or $(1,2)$ to the states at 2.839.9, 3000.7, 3250.4, 3383.4, and 3412.8 keV. These

levels may correspond to the states at 2840, 3003, 3249 (2^+), 3376 (3^-), and 3414 (3^-) keV in the present study, respectively. The levels obtained with the other studies²⁰ such as in-beam spectroscopies, Coulomb excitation, and β decays are different levels from the results of the present study, except for the lower levels.

^{80}Se : Previously, ^{80}Se was studied with the (p,p') reaction by Darcey *et al.*³³ Unfortunately the energy resolution of these studies (50–100 keV) was not enough to separate higher excited states. Most of the levels above 2.5 MeV excitation energy listed in Table VI are newly observed in the present experiment. The 2^+ states in 1.871 and 1.960 MeV observed in the present study are in good agreement with the results²¹ of the studies of the (γ,γ') reaction, Coulomb excitation, and β decay of ^{80}As .

^{82}Se : There are several studies^{22,34} with the inelastic scattering, the (t,p) reaction, and the β decay of ^{82}As . The lower levels have been assigned in ^{82}Se at 0.654 (2_1^+),

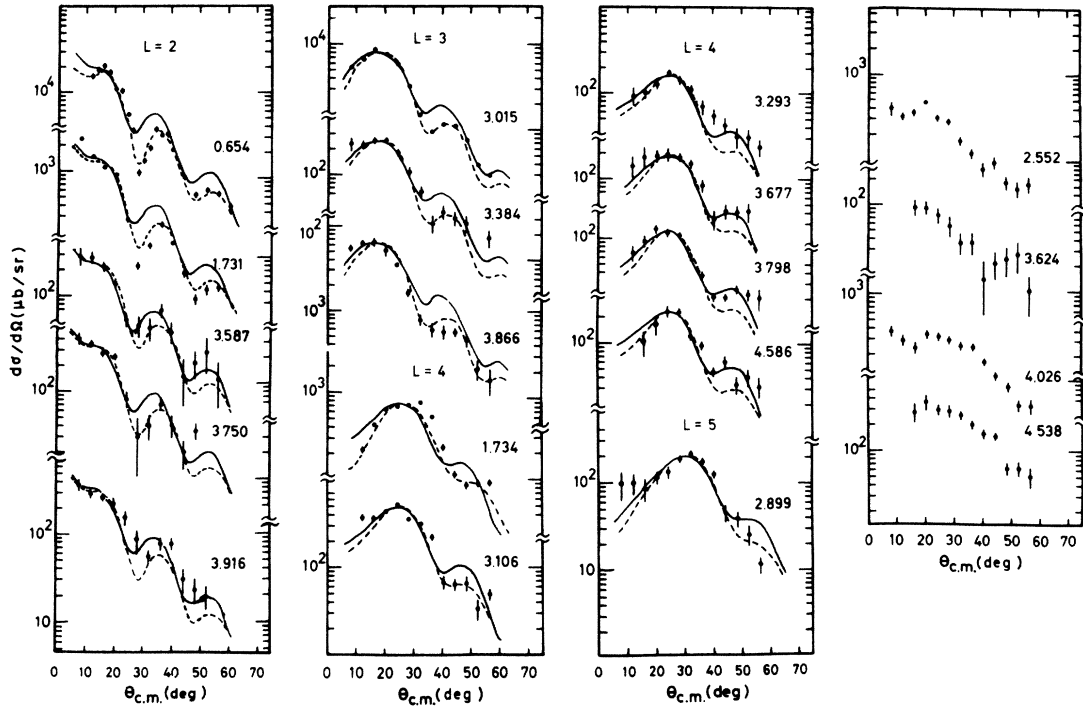


FIG. 11. Angular distributions of protons from the $^{82}\text{Se}(p,p')$ reaction. See also the caption for Fig. 7.

1.731 (2_2^+), and 1.734 (4_1^+) MeV, and several levels such as 3_1^- were tentatively proposed. Recently, Watson *et al.*²² have studied ^{82}Se with the $^{80}\text{Se}(t,p)^{82}\text{Se}$ reaction at 15 MeV, and 24 levels have been identified up to approximately 5.0 MeV excitation as listed in Table VII. The levels at 3.106 (4^+), 3.587 (2^+), 3.750 (2^+), and 4.586 (4^+) MeV in the present study may correspond to the levels at 3.101 (5^-), 3.581 (2^+), 3.748 (2^+), and 4.587 (4^+) MeV studied by Watson *et al.*²² The 5^- level at 2.893 MeV obtained in the present study may correspond to the 2.893 MeV level assigned tentatively $J^\pi = (4^-)$ by Kratz *et al.*³⁵

2. Systematics of 2^+ strengths

The 2^+ states observed in this study are distributed in the lower excitation energy. The lowest 2_1^+ states were strongly excited in all Se isotopes. Several 2^+ states above the excitation energy of the 2_1^+ state were observed with small transition strengths (less than about 1.0 spu). The transition strengths for these 2^+ states in the EWSR fraction are presented in Table VIII. The observed EWSR fraction of the 2^+ states in the energy region $E_x = 0.5\text{--}4.0$ MeV was about 11.4% for ^{74}Se , 11.5% for ^{76}Se , 11.3% for ^{78}Se , 8.0% for ^{80}Se , and 6.8% for ^{82}Se , respectively.³⁶

3. Systematics of 3^- strengths

The 3^- states observed in this study were distributed in the 2.5–5.0 MeV region which was below the expected

low energy octupole resonance (LEOR).³⁷ The transition strengths of the 3^- states in the EWSR fraction are presented in Table IX. As seen in the table, the lowest 3^- states were strongly excited. The strength for the 3_2^+ state was rather strong only in ^{74}Se and those for the higher 3^- states in all Se isotopes were weakly observed. The summed strengths of the higher 3^- states above the 3_1^- states were observed with 30–40% of the total strengths measured in the $E_x = 2.5\text{--}5.0$ MeV region. The EWSR fraction in the energy region $E_x = 2.0\text{--}5.0$ MeV is about 10.2% for ^{74}Se , 9.0% for ^{76}Se , 8.3% in ^{78}Se , 8.3% for ^{80}Se , and 7.3% for ^{82}Se , respectively.

4. Systematics of 4^+ strengths

Contrary to the distribution of the transition strengths for the 3^- states where the 3_1^- state has large collectivity, the 4^+ states split into many states with comparable strengths in the $E_x = 2.5\text{--}5.0$ MeV region. The transition strengths of the 4^+ states in the EWSR fraction are presented in Table X. Except for ^{82}Se , the strengths of the first 4^+ states are rather weak in Se compared to those of the higher-excited 4^+ states in which the strongest one has a strength of almost 3.0 spu. The observed EWSR fraction of the 4^+ states is about 2.6% for ^{74}Se , 3.7% in ^{76}Se , 1.8% for ^{78}Se , 1.4% for ^{80}Se , and 1.3% for ^{82}Se , respectively.

TABLE XI. The energy gaps (Δ_p for proton and Δ_n for neutron) and the interaction strengths (ξ_L) used in the present calculations.

Nuclei	Energy gaps (MeV)		Interaction strengths (ξ_L)		
	Δ_p	Δ_n	ξ_2	ξ_3	ξ_4
^{74}Se	1.60	1.18	0.82	0.77	0.77
^{76}Se	1.63	1.37	0.82	0.77	0.77
^{78}Se	1.47	1.30	0.82	0.77	0.65
^{80}Se	1.47	1.13	0.82	0.77	0.65
^{82}Se	Set I	1.55	0.82	0.77	0.40
	Set II	1.27	0.68	0.77	0.65

B. Comparison of the experimental results with the RPA calculations

1. General description of RPA calculations

In the present study, the RPA calculations with pairing plus quadrupole-quadrupole (2^+), octupole-octupole (3^-), and hexadecapole-hexadecapole (4^+) interactions for spherical nuclei were performed with the code by Kishimoto.³⁸ The RPA calculations in spherical nuclei have several parameters: (1) pairing energies (Δ_p for proton and Δ_n for neutron); (2) single particle energies (ϵ_j); (3) interaction strength (ξ_L) defined in the unit of the self-consistent strength,³⁹

$$\chi_L^{\text{self}} = \frac{4\pi}{2\lambda+1} \frac{M\omega_0^2}{A \langle r^{2\lambda-2} \rangle}$$

for interaction

$$-\frac{1}{2} \sum_{L=2,3,4} \chi_L \sum_{\mu} \sum_{i,j=1}^A (r^\lambda Y_{\lambda\mu})_i^\dagger (r^\lambda Y_{\lambda\mu})_j,$$

where χ_L is $\xi_L \chi_L^{\text{self}}$; (4) the values of isoscalar effective charges for proton and neutron which are fixed to 1.0, because all major shells are used and thus all transitions are included in these calculations. These parameters were determined to reproduce well the excitation energies and

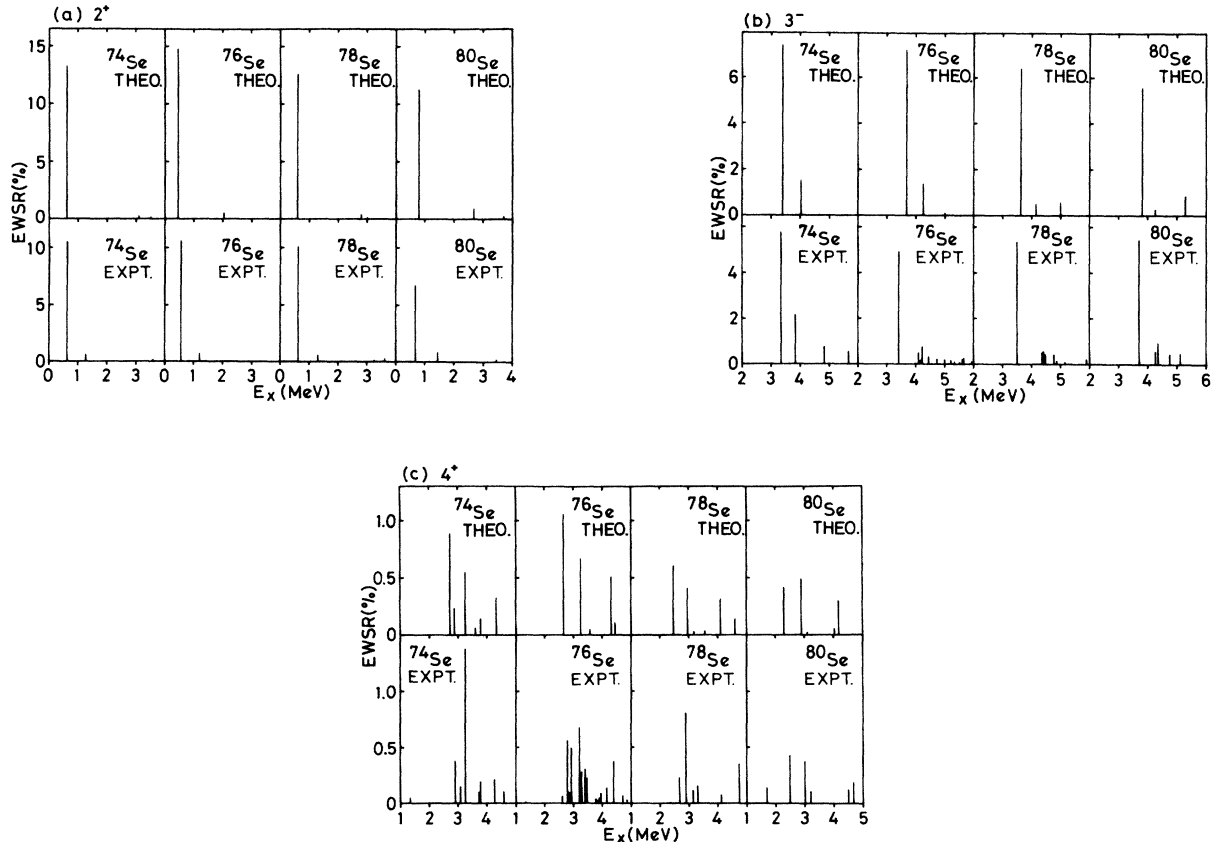


FIG. 12. The energy weighted sum-rule (EWSR) fractions for the (a) 2^+ , (b) 3^- , and (c) 4^+ states in $^{74-80}\text{Se}$ nuclei. The theoretical predictions from the RPA calculations are shown in the upper part of the figure.

TABLE XII. The single particle energies (ϵ_j) of the $2p_{3/2}$, $1f_{5/2}$, $2p_{1/2}$, and $1g_{9/2}$ shells and chemical potential (λ) used in the present calculations.

Nuclei	ϵ_j and λ (proton shells) (MeV)					ϵ_j and λ (neutron shells) (MeV)					
	$2p_{3/2}$	$1f_{5/2}$	$2p_{1/2}$	$1g_{9/2}$	λ	$2p_{3/2}$	$1f_{5/2}$	$2p_{1/2}$	$1g_{9/2}$	λ	
⁷⁴ Se	0.24	1.06	1.16	1.84	0.32	-2.59	-1.25	-0.11	0.43	-0.47	
⁷⁶ Se	0.24	1.06	1.22	1.84	0.29	-3.10	-2.10	-1.99	-0.72	-1.09	
⁷⁸ Se	0.23	0.95	1.18	1.80	0.32	-4.20	-2.87	-2.58	-1.75	-1.66	
⁸⁰ Se	0.23	0.75	1.14	1.76	0.23	-4.90	-3.62	-3.25	-2.34	-1.94	
⁸² Se	Set I	0.23	0.64	1.11	1.72	0.14	-5.25	-4.64	-3.54	-3.46	-2.17
	Set II	0.23	1.11	1.74	2.52	0.82	-5.70	-4.35	-4.29	-2.27	-1.74

transition strengths for the low-lying 2^+ , 3^- , and 4^+ states, as well as those of the giant quadrupole, octupole, and hexadecapole states.

The pairing energies used in the present calculations are listed in Table XI. The Δ_p values obtained are somewhat lower than those predicted by the binding energy relation and close to the values calculated by using the empirical formula studied by Vogel *et al.*⁴⁰ The Δ_n values used are different from their systematics, because neutron numbers of Se nuclei are close to the magic number ($N = 50$).

The single particle energies ϵ_j are corrected for $1f_{5/2}$, $2p_{1/2}$, and $1g_{9/2}$ shells to some extent (within 1.5 MeV) from those obtained with an ordinary Nilsson potential⁴¹ and are listed in Table XII, together with a chemical potential λ . The ϵ_j values used are roughly consistent with those obtained from single-nucleon transfer reactions⁴² and those of the $1f_{5/2}$ shell lie between $2p_{3/2}$ and $2p_{1/2}$ shell energies in all Se isotopes in the present calculations.

The interaction strengths ξ_L were fixed for all the isotopes studied in the case of the 2^+ and 3^- states, but were

changed slightly in the case of the 4^+ states. The values used are also listed in Table XI, and are almost the same values as those in the previous work.¹³ In the case of ⁸²Se, two sets of the parameter are used, because the previous parameters for the RPA prediction¹³ do not reproduce the excitation energy and the EWSR fraction for the 2_1^+ state.

The excitation energies and EWSR fractions of the 2^+ , 3^- , and 4^+ states in ^{74–82}Se calculated with these parameters are presented in Figs. 12(a)–(c) and 13, and also compared with the experimental results. The calculated EWSR fractions of the giant quadrupole, octupole, and hexadecapole resonances for ^{74–82}Se using the same parameters are also listed in Table XIII. They are in reasonable agreement with those expected from the experimental systematics obtained for medium- A nuclei.⁴³

2. The 2^+ strengths

The calculated excitation energies of the 2^+ states are in fairly good agreement with the experimental results in ^{74–80}Se isotopes, but the 2_2^+ states lie higher than the experimental ones. The calculated strengths for the 2_1^+ states are somewhat stronger (factor of about 1.5) than the experimental ones as shown in Fig. 12(a) and Table XIV. In the case of ⁸²Se, the excitation energies and strengths of the 2_1^+ and 2_2^+ states are well reproduced by the calculations using the parameter set II as shown in Fig. 13 and Table XIV.

3. The 3^- strengths

The one-phonon octupole states in ^{76–82}Se have been investigated by Matoba *et al.*¹¹ and the excitation energies and transition strengths for the 3_1^- states have been rather well predicted by the pairing plus octupole-octupole model by Veje.⁴⁴ The disagreement between Veje's predictions and the present experimental results becomes, however, remarkable in the higher octupole states, where the predicted excitation energies and strengths for the 3_2^- states are much higher and larger.

On the other hand, the present calculation gives a good description for the states up to higher excitation energies as well. The excitation energies and strengths for the LEOR are also well reproduced as listed in Table XIII.

4. The 4^+ strengths

Goswami and Lin¹⁰ have calculated the excitation energies and transition strengths for the 4^+ states with a

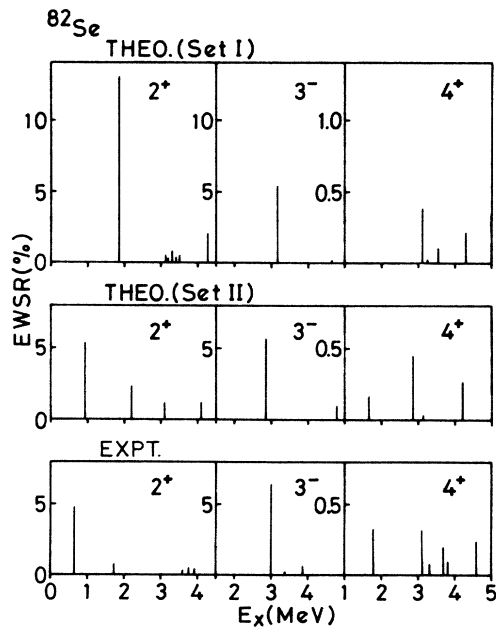


FIG. 13. The energy weighted sum-rule (EWSR) fractions for the 2^+ , 3^- , and 4^+ states in ⁸²Se. The theoretical predictions from RPA calculations using two parameter sets listed in Table XII are shown in the upper part of figure.

TABLE XIII. The excitation energies and EWSR fractions for the giant resonances in the present calculations using the same parameters listed in Table XII.

Nuclei		2 ⁺		3 ⁻ (LEOR)		4 ⁺	
		E_x (MeV)	EWSR (%)	E_x (MeV)	EWSR (%)	E_x (MeV)	EWSR (%)
⁷⁴ Se		13.0–16.0	56.8	6.5–8.5	14.3	14.5–17.5	16.3
⁷⁶ Se		13.0–16.0	55.9	6.5–8.5	15.4	14.5–17.5	16.4
⁷⁸ Se		13.0–16.0	58.6	6.5–8.5	15.5	14.5–17.5	16.2
⁸⁰ Se		13.0–16.0	59.4	6.5–8.5	15.1	14.5–17.5	15.6
⁸² Se	Set I	12.5–15.5	48.9	6.5–8.5	15.6	14.0–17.0	12.1
	Set II	12.5–15.5	57.5	6.5–8.5	16.7	14.0–17.0	16.6

surface-delta interaction for the even-even Zn, Ge, Se, and Te isotopes, and have predicted that the lowest hexadecapole vibrational state has a $B(E4)$ of around 10 sp μ which exhausts 1–3 % of the EWSR. The experimental results⁷ on the low-lying 4⁺ states in ^{64–68}Zn are in essential agreement with their prediction.

In this study, the summed EWSR fraction of the 4⁺ states increase with decreasing neutron number from ⁸²Se (1.3%) up to ⁷⁶Se (3.6%) and then decrease in ⁷⁴Se (2.6%). Strong fragmentations occur in the excitation energy of about 2–4 MeV for ⁷⁶Se. These features are in disagreement with the prediction of Goswami and Lin.

The strong fragmentations of the hexadecapole vibrational strengths observed in ^{74–82}Se are well reproduced by the present RPA calculations as shown in Figs. 12(c) and 13. The hexadecapole giant resonances are also distributed in the excitation energy of about 14–17 MeV. The EWSR fraction of the 4⁺ states in ⁸²Se is discussed in detail in the next subsection.

5. RPA calculation in ⁸²Se

Previously, the hexadecapole strengths in ⁸²Se were calculated with the values for the energy gaps ($\Delta_p=1.55$ MeV and $\Delta_n=1.35$ MeV) and the interaction strength ($\xi_4=0.40$) listed in Table X (set I).¹³ In these calculations, Δ_p and Δ_n values for ⁸²Se are larger than those for ^{78,80}Se. Generally, Δ_p and Δ_n values slowly decrease with increasing A or asymmetry⁴⁰ $(N-Z)/A$, and Δ_n values are smaller when neutron numbers are close to the magic

number. The RPA calculations in ⁸²Se are therefore performed by using two parameter sets (sets I and II) as listed in Table X and the results are presented in Fig. 13. Set I are the same parameters studied previously,¹³ and set II are the new parameters added in the present analyses.

By using the parameter set I, good agreements with the experimental results for the excitation energies and for the strengths of the 3⁻ and 4⁺ states are obtained, while the agreements with the 2₁⁺ states become worse than those in the case of ^{74–80}Se nuclei. In the case of parameter set II, in addition to the 3⁻ and 4⁺ states,¹³ those of the 2₁⁺, 2₂⁺, and 4₁⁺ states are also well reproduced as shown in Fig. 13 and Table XIV. These features suggest that the lowest hexadecapole vibrational state in ⁸²Se is lower in the excitation energy than those of the other Se isotopes and occupies with large components in the 4₁⁺ state.

V. SUMMARY

A large number of new levels in ^{74–82}Se nuclei were observed in the excitation energy up to 4.8–5.5 MeV with the present (p,p') reaction at 64.8 MeV. Shapes of the angular distributions for these states are well reproduced by the DWBA and CC calculations, and thus allowed us to assign spin parity to most of the levels.

Many 3⁻ and 4⁺ levels with appreciable strengths were observed for the first time in the energy region from 2.5 to 5.0 MeV. Several 5⁻ levels were also observed for the first time.

The results of the RPA predictions for the 2⁺, 3⁻, and 4⁺ states in ^{74–82}Se are in reasonable agreement with the

TABLE XIV. The EWSR fractions for the 2⁺, 3⁻, and 4⁺ states of ^{74–82}Se nuclei in the energy range $E_x=0.5-4.0$ MeV for the 2⁺ states and $E_x=1.0-5.0$ MeV for the 3⁻ and 4⁺ states observed in the present experiments (Expt.). The RPA predictions on the EWSR fractions are also listed (Theo.).

Nuclei		EWSR (2 ⁺)		EWSR (3 ⁻)		EWSR (4 ⁺)	
		Expt.	Theo.	Expt.	Theo.	Expt.	Theo.
⁷⁴ Se		11.40	14.09	9.37	9.02	2.59	2.22
⁷⁶ Se		11.54	15.61	8.14	8.75	3.58	2.39
⁷⁸ Se		11.31	11.39	7.89	7.56	1.75	1.76
⁸⁰ Se		7.99	12.75	7.98	7.03	1.38	1.46
⁸² Se	Set I	6.79	13.28	7.33	5.62	1.27	0.73
	Set II	6.79	8.09	7.33	6.70	1.27	1.02

observed excitation energies and strengths. The fragmentations and distributions of the hexadecapole vibrational strengths observed in ^{74–82}Se are generally well reproduced by the RPA calculations. As for the 4_1^+ state in ⁸²Se, the experimental results show that the deformation parameter obtained is large and the EWSR fraction is largest in several 4^+ states observed. And the present RPA predictions suggest that the 4_1^+ state in ⁸²Se has large components of the hexadecapole vibrational state, in contrast to the other Se nuclei.

As discussed in the Introduction, the Se isotopes show transitional features where the couplings between various degrees of freedom must play on important roles, especially in the case of ⁷⁶Se, where large fragmentations of the octupole and hexadecapole transition strengths are observed. More experimental efforts should be extended to

pin down such coupling schemes by using various types of reactions, and at the same time more detailed analyses are needed to clarify these features using other theoretical models such as the interacting boson model⁴⁵ including the g boson in addition to the s and d bosons.

ACKNOWLEDGMENTS

The author wishes to thank Prof. T. Yanabu, Prof. S. Matsuki, and Prof. T. Kishimoto for valuable discussions and encouragements during this work. The author expresses his thanks to Dr. N. Sakamoto, Dr. T. Higo, and Dr. Y. Okuma and Mr. Y. Kadota for their helpful cooperation. It is a pleasure to acknowledge the construction members of RAIDEN and the cyclotron crew of RCNP for their kind support and cooperation.

-
- ¹J. H. Hamilton, A. V. Ramayya, W. T. Pinkston, R. M. Ronninger, G. Garcia-Bermudez, R. L. Robinson, H. J. Kim, and R. O. Sayer, *Phys. Rev. Lett.* **32**, 239 (1974); J. H. Hamilton, H. L. Crowell, R. L. Robinson, A. V. Ramayya, W. E. Collins, R. M. Ronningers, V. Haruhn-Rezwani, J. A. Maruhn, N. C. Singhal, H. J. Kim, R. O. Sayer, T. Magee, and L. C. Whitlock, *ibid.* **36**, 340 (1976).
- ²D. Ardouin, R. E. Brown, J. A. Cizewski, E. Flynn, and J. W. Sinier, *Phys. Rev. C* **22**, 432 (1980).
- ³N. Sakamoto, S. Matsuki, K. Ogino, Y. Kadota, T. Tanabe, and T. Okuma, *Phys. Lett.* **83B**, 39 (1979).
- ⁴S. Matsuki, T. Higo, T. Ohsawa, T. Shiba, T. Yanabu, K. Ogino, Y. Kadota, K. Haga, N. Sakamoto, K. Kume, and M. Matoba, *Phys. Rev. Lett.* **51**, 1741 (1983).
- ⁵S. Matsuki, K. Ogino, Y. Kadota, N. Sakamoto, T. Tanabe, M. Yasue, A. Yokomizo, S. Kubono, and Y. Okuma, *Phys. Lett.* **113B**, 21 (1982); S. Matsuki, N. Sakamoto, K. Ogino, Y. Kadota, Y. Saito, T. Tanabe, M. Yasue, and Y. Okuma, *ibid.* **72B**, 319 (1978).
- ⁶J. P. Delaroche, R. L. Varner, T. B. Clegg, R. E. Anderson, B. L. Burks, E. J. Ludwig, and J. F. Wilkerson, *Nucl. Phys.* **A414**, 113 (1984).
- ⁷N. Alpert, E. Marteus, and W. Pickles, *Phys. Rev. C* **4**, 1230 (1971).
- ⁸M. Koike, I. Nonaka, J. Kokame, H. Kamitsubo, Y. Awaya, T. Wada, and H. Nakamura, *Nucl. Phys.* **A125**, 161 (1969).
- ⁹J. F. Ziegler and G. A. Peterson, *Phys. Rev.* **165**, 1337 (1968).
- ¹⁰A. Goswami and L. Lin, *Phys. Lett.* **42B**, 310 (1972).
- ¹¹M. Matoba, M. Hyakutake, N. Koori, Y. Irie, and Y. Aoki, *Nucl. Phys.* **A325**, 389 (1979).
- ¹²T. H. Curtis, H. F. Lutz, and W. Bartolini, *Phys. Rev. C* **1**, 1418 (1970).
- ¹³K. Ogino, Y. Kadota, H. Haga, S. Matsuki, T. Higo, T. Shiba, N. Sakamoto, Y. Okuma, and T. Yanabu, *Phys. Lett.* **130B**, 147 (1983).
- ¹⁴H. Ikegami, S. Morinobu, I. Katayama, M. Fujita, and S. Yamabe, *Nucl. Instrum. Methods* **175**, 445 (1980).
- ¹⁵Y. Fujita, K. Nagayama, S. Morinobu, M. Fujita, I. Katayama, T. Yamazaki, and H. Ikegami, *Nucl. Instrum. Methods* **173**, 265 (1980).
- ¹⁶J. Raynal (private communication).
- ¹⁷P. D. Kunz (private communication).
- ¹⁸D. C. Kocher, *Nucl. Data. Sheets* **17**, 519 (1976).
- ¹⁹F. E. Bertrand and R. L. Auble, *Nucl. Data. Sheets* **19**, 509 (1976).
- ²⁰B. Singh and D. A. Viggars, *Nucl. Data. Sheets* **33**, 189 (1981).
- ²¹B. Singh and D. A. Viggars, *Nucl. Data. Sheets* **36**, 127 (1982).
- ²²D. L. Watson, M. D. Cohler, and H. T. Fortune, *Phys. Rev. C* **30**, 826 (1984).
- ²³N. Yoshikawa, Y. Shida, O. Hashimoto, M. Sakai, and T. Numao, *Nucl. Phys.* **A327**, 477 (1979).
- ²⁴P. B. Piercey, A. V. Ramayya, R. M. Ronninger, J. H. Hamilton, V. Maruhn-Rezwani, R. L. Robinson, and H. J. Kim, *Phys. Rev. C* **19**, 1344 (1979).
- ²⁵H. Orihara, M. Takahashi, Y. Ishizaki, T. Suehiro, K. Miura, Y. Hiratate, and H. Yamaguchi, *Nucl. Phys.* **A267**, 276 (1976).
- ²⁶M. Borsaru, D. W. Gebbie, J. Nurzynski, C. L. Hollas, L. O. Barbopoulos, and A. R. Quinton, *Nucl. Phys.* **A287**, 379 (1977).
- ²⁷R. Kaur, A. K. Sharma, S. S. Sood, H. R. Verma, and P. N. Trehan, *J. Phys. Soc. Jpn.* **49**, 1214 (1980).
- ²⁸R. Lecomte, P. Paradis, G. Lamoureux, and S. Monaro, *Nucl. Phys.* **A284**, 123 (1977).
- ²⁹S. Matsuzaki and H. Taketani, *Nucl. Phys.* **A390**, 413 (1982).
- ³⁰J. C. Wells, R. L. Robinson, H. J. Kim, R. O. Sayer, R. B. Piercey, A. V. Ramayya, J. H. Hamilton, and C. F. Maguire, *Phys. Rev. C* **22**, 1126 (1980).
- ³¹Y. Tokunaga, H. Seyfarth, W. Schult, H. Borner, C. Hofmeyer, G. Barreau, R. Brissot, U. Kaup, and C. Monkemeyer, *Nucl. Phys.* **A411**, 209 (1983).
- ³²P. F. Hinrichsen, G. Kennedy, and T. Paradellis, *Nucl. Phys.* **A212**, 365 (1973).
- ³³W. Darcey, D. J. Pullen, and N. W. Janner, in *Proceedings of the International Conference on Direct Interactions and Nuclear Reaction Mechanisms, Pudna, 1962*, edited by E. Clemental and C. Villi (Gordon and Breach, New York, 1963), p. 795.
- ³⁴J. F. Lemming and R. L. Auble, *Nucl. Data. Sheets* **15**, 315 (1975).

- ³⁵J. V. Kratz, H. Franz, N. Kaffrell, and G. Herrmann, Nucl. Phys. **A250**, 13 (1975).
- ³⁶A. M. Bernstein, *Advances in Nuclear Physics*, edited by M. Baranger and E. Vogt (Plenum, New York, 1969), Vol. III, p. 325.
- ³⁷M. K. Kirson, Phys. Lett. **108B**, 237 (1982); and references therein.
- ³⁸T. Kishimoto (private communication).
- ³⁹A. Bohr and B. R. Mottelson, *Nuclear Structure* (Benjamin, Reading, MA, 1975), Vol. 2, Chap. 6.
- ⁴⁰P. Vogel, B. Jonson, and P. G. Hansen, Phys. Lett. **139B**, 227 (1984).
- ⁴¹S. G. Nilsson, C. F. Tsang, A. Sobiczewski, I. L. Lamm, P. Moller, and B. Nilson, Nucl. Phys. **A131**, 1 (1969).
- ⁴²J. D. Zumbro, R. W. Tarara, and C. P. Browne, Nucl. Phys. **A393**, 15 (1983).
- ⁴³F. E. Bertrand, Nucl. Phys. **A345**, 153 (1981), and references therein.
- ⁴⁴C. J. Veje, K. Dan. Vidensk. Selsk. Mat.-Fys. Medd. **35**, No. 1 (1966).
- ⁴⁵A. Arima and F. Iachello, Ann. Phys. (N.Y.) **111**, 201 (1978)